



# Effect of Glaze Composition and Sintering Process on the Pyroplastic Deformation Behaviour of Bone China

Fazilet GÜNGÖR<sup>1</sup> and Berda ALTUN<sup>2</sup>

<sup>1</sup>Porser Porselen ve Seramik San. Tic. Ltd. Şti., Sancaktepe, İstanbul

<sup>2</sup>Kütahya Porselen, R&D Center, Kütahya/ Turkey

**Sorumlu Yazar / Corresponding Author**

Fazilet GÜNGÖR

fazilet.gungor@porser.com.tr

**Makale Bilgisi / Article Info**

Sunulma / Received : 02.06.2020

Düzeltilme / Revised : 06.08.2020

Kabul / Accepted : 17.08.2020

**Destekleyen Kuruluş / Funding Agency**

**Anahtar Kelimeler**

Bone China

Sır

Bünye

Kompozisyon

SiO<sub>2</sub>/Al<sub>2</sub>O<sub>3</sub>

**Keywords**

Bone China

Glaze

Body

Composition

SiO<sub>2</sub>/Al<sub>2</sub>O<sub>3</sub>

**ORCID**

Fazilet Güngör

<https://orcid.org/0000-0002-2405-0358>

## Abstract

In this paper, the effect of composition of the glaze and the sintering process on the pyroplastic deformation of bone china was investigated. Besides the glaze composition and heating cycle, the other parameters that affect the pyroplastic deformation such as body composition, body and glaze density and thickness were kept at the constant values. In the glaze composition, the rate of SiO<sub>2</sub>/Al<sub>2</sub>O<sub>3</sub> was changed from 8.58 to 11.20, the amount of Na<sub>2</sub>O, K<sub>2</sub>O, CaO and MgO were kept at the constant values. The melting behavior of the glazes was examined by heat microscopy. The phases were determined by X-ray diffraction. Pyroplastic deformation and thermal expansion measurements were taken on the samples. Morphological and chemical characteristics of the samples was investigated by SEM and EDX, respectively. The pyroplastic deformation of the samples increased as the rate of SiO<sub>2</sub>/Al<sub>2</sub>O<sub>3</sub> increased in the glaze composition due to the changes in the microstructure of the body such as the dissolution of the crystals and increasing the amount of the glassy phase and increasing the thickness of interlayer between the glaze and the body.

## Sır Kompozisyonu ve Sinterleme Sürecinin Bone China Bünye Pyroplastik Deformasyon Davranışına Etkisi

### Özet

Bu çalışmada, sır kompozisyonunun ve sinterleme sürecinin pyroplastik deformasyon davranışı üzerine etkileri incelenmiştir. Sır kompozisyonu ve ısı çevrim süreci dışındaki, pyroplastik deformasyon davranışını etkileyebilecek olan; bünye kompozisyonu, sır ve bünye yoğunluk ve kalınlıkları gibi parametreler sabit tutulmuştur. Sır bileşiminde SiO<sub>2</sub>/Al<sub>2</sub>O<sub>3</sub> oranı 8.58-11.20 aralığında değiştirilirken Na<sub>2</sub>O, K<sub>2</sub>O, CaO ve MgO içeriği sabit değerlerde tutulmuştur. Sırların ergime davranışları ısı mikroskobu ile incelenmiştir. Mikroyapıda oluşan fazlar XRD analizi ile tespit edilmiştir. Numunelerin morfolojik ve kimyasal karakteristikleri ve kimyasal bileşimleri sırasıyla, SEM ve EDX analizleri ile incelenmiştir. Numunelerin pyroplastik deformasyonu sır kompozisyonunda SiO<sub>2</sub>/Al<sub>2</sub>O<sub>3</sub> oranı arttıkça artmıştır. Çalışma verileri bu sonucun sır kompozisyonunda SiO<sub>2</sub>/Al<sub>2</sub>O<sub>3</sub> oranının artması ile mikroyapıda oluşan kristallerin çözünmesi, cam faz miktarının artışı ve sır-bünye ara tabaka kalınlığının artışı ile ilgili olduğunu göstermiştir.

## 1. INTRODUCTION

Bone China is a highly specialized product in terms of its appearance; being exceptionally white and translucent makes it the world's most expensive type of tableware [1]. It is a highly crystalline white-ware that exhibits good resistance to edge chipping and high flexural strength. During firing, the deformation of white-ware may have a complex origin because of its polycrystalline microstructure. In the case of glazed ware the interrelation between the glaze and the body during the heat treatment process must be considered. The main interrelation factors are; 1- the tension, because of the difference of thermal expansion of the body and the glaze, 2- thickness of the glaze and 3- development of interlayer, as a result of diffusion and dissolution phenomena between the glaze and the body. Thus glaze and body do not behave as independent layers because of the presence of such an interlayer, which affects the properties of the final product [2, 3]. A wide interface indicates a substantial dissolution of the body by the glaze and vice versa. Also the glaze-body interlayer may be higher or lower in thermal expansion than the glaze or the body due to localized variations, e.g. quartz grains at the interface [4]. The reaction at the interlayer must be sufficient to hold the glaze to the body. The amount of glaze penetration also affects glaze fit. The amount of penetration can vary drastically and depends chiefly on the glaze and body composition and the characteristics of them, such as particle size and distribution, the thickness of the glaze and the amount, size and the morphology of the pores [2].

As the gloss firing approaches its peak temperature, the glassy phase's viscosity in the interlayer between glaze and the body decreases as a result of the changed composition of the interlayer due to the reaction between glaze and body. It should not be so low as to cause distortion by the gravitational effect during the sintering process. Viscosity should be in the appropriate value to provide higher surface stress than the gravity force's stresses. Viscous liquid silicate forms at the firing temperature and acts as a binder for the body. The amount and viscosity of the liquid phase should be acceptable and sufficient for densification. In excess amount and formation of vitreous glassy phase, slippage occurs between the particles.

As the temperature increases, the amount of glassy phase increases and viscosity decreases. Due to the increased amount of glassy phase and decreased of its viscosity, creep behavior accelerates and causes the product to deform. [5-7].

In this study, effect of the composition of the glaze and the sintering process on the pyroplastic deformation of bone china was investigated. Except for the glaze composition and heating cycle, the other parameters that effects the pyroplastic deformation such as body composition, body and glaze density and thickness were kept at the constant values. The results were evaluated and interpreted considering the affect of the glaze composition on the pyroplastic behavior of the product.

The aim of this study is to determine the effect of glaze composition and sintering process on the pyroplastic deformation behaviour of bone china and to explain the reasons of the changed behaviour.

## 2. METHODS

Bone china body composition was studied according to the literature review [7] and developed by the experimental studies. Chemical analysis and average particle size (d(0.5)) results of the raw materials for bone china body and glaze compositions were given in Table 1. The chemical results of the raw materials were determined by the X-ray fluorescence method using X Lab 2000-Spectro and the particle size distribution of the raw materials were measured by diffraction method using Malvern Master Sizer 2000 G model. Since the raw materials were used in ground form, the mixtures were prepared in a mixer without milling. Bone ash, albite, K-feldspar, quartz and clay were used in the body composition. The chemical composition of the bone china body was given in Table 2. Raw materials were dispersed in an aqueous solution to prepare the batches. Slip that containing 70 wt percentage solids and 0.015 wt percentage dispersant (Na-silicate) was mixed for 1 h using IKA RW 20 digital mixer. The slurries were screened by 60 mesh (250 µm) sieves. Slips were poured into the bar shaped plaster molds. The dimension of the bars was 3.5 cm×20 cm×1 cm.

**Table 1.** Chemical analysis and average particle size [d(0.5)] results of the raw materials used for body and glaze

	SiO <sub>2</sub>	Al <sub>2</sub> O <sub>3</sub>	Fe <sub>2</sub> O <sub>3</sub>	CaO	MgO	Na <sub>2</sub> O	K <sub>2</sub> O	TiO <sub>2</sub>	SO <sub>3</sub>	P <sub>2</sub> O <sub>4</sub>	L.O.I.	d(0.5) µm
Bone Ash	2.3	1.2	0	55.2	0.1	0.2	0	0	0	40.9	0.1	5.24
K-Feldspar	68.9	20.5	0.1	0.4	0.2	0.1	9.6	0	0	0	0.2	4.28
Kaolin	49.3	36.1	0.3	0.1	0.1	0.1	0	0.1	0.1	0	13.9	3.15
Clay	51	35	0.3	0.2	0.1	0.1	0.3	0.2	0	0	12.9	2.45
Quartz (for glaze)	97.7	1.2	0.2	0.2	0	0.1	0.3	0	0	0	0.2	3.92
Quartz (for body)	97.7	1.2	0.2	0.2	0	0.1	0.3	0	0	0	0.2	14.12
Albite	67.6	19.4	0.1	0.4	0.2	11.8	0.2	0	0	0	0.2	4.52
Whiting	0.8	0	0	55.6	0.5	0.1	0	0	0.1	0	42.8	5.19
Dolomite	0	0	0	36.6	17.1	0	0	0	0.1	0	45.6	4.87

The whole substrates were shaped in the same dimensions and densities for eliminating the parameters of the thickness and densities. After shaping, substrates were biscuit fired at 1000 °C to increase their strength for experimental studies such as glazing and transporting to the kiln. Initial glaze recipe was also developed by experimental studies and its rate of SiO<sub>2</sub>/Al<sub>2</sub>O<sub>3</sub> was changed. Commercial quartz, albite, K- feldspar, whiting (CaCO<sub>3</sub>), dolomite and kaolin samples were used to produce six glazes. Seger analyses of the glazes were given in Table 3. After accurate weighing of all raw materials, carboxyl methyl cellulose (CMC), sodium tripolyphosphate (STPP) and water were mixed in a jet mill for 15 min. Glazes were applied to biscuit fired bone china body by spray gun at the density of 1.40-1.41 gr/cm<sup>3</sup> and in the thickness of 400 µm. The thickness of the glazes was measured by a pocked pen microscope (e.j. payne ceramic, X50, MIC050). Whole glazes were applied in the same density and thickness for eliminating the effect of thickness and density on the pyroplastic deformation of glaze.

Heat microscopy analyses of the prepared glazes were investigated using Misura 3.32-ODHT-HSM 1600/80 (Expert System Solutions) brand and model using a dual-cam contactless optical dilatometer. The measurement was carried out at a temperature of 1400 °C for 30 minutes and at a total firing time of 180 minutes. Glazed samples were fired in the laboratory type kiln with two different sintering parameters coded HT01 and HT02. For HT01; heating rate was 10 kmin<sup>-1</sup>, dwelling temperature was 1250 °C and the dwelling time was 40 minutes. For HT02; heating rate was 10 kmin<sup>-1</sup>, dwelling temperature was 1250 °C and the dwelling time was 80 minutes. The viscosities of the glassy phases were calculated according to Lakatos [8]. Viscosity of the glassy phase was calculated at the maximum temperature that the samples exposed. The maximum temperatures that the samples exposed were determined by the seger rings (Ferro, STH 291). The maximum exposed temperature was 1258 °C for HT01 and 1264 °C for HT02. Pyroplastic deformation of the samples was measured as indicated Conserva at all [9]. The pyroplastic index (PI) of each samples was determined by three point test method after firing: where h is the thickness of the body, S the maximum deflection and L the distance between the refractory supports as indicated in Fig. 1.

$$PI = \frac{4h^2}{3L^4} S \quad (1)$$

**Table 2.** Bone China body composition (wt%)

	SiO <sub>2</sub>	Al <sub>2</sub> O <sub>3</sub>	Fe <sub>2</sub> O <sub>3</sub>	CaO	MgO	Na <sub>2</sub> O	K <sub>2</sub> O	SO <sub>3</sub>	TiO <sub>2</sub>	P <sub>2</sub> O <sub>4</sub>	L.O.I.
Bone China Body	35.8	21.4	0.2	19.5	0.1	0.2	1.6	0.1	0.1	14.3	-

The detection of the phases formed in the fired product was carried out with a Rigaku Rint 2000 XRD device. For microstructural examinations, secondary electron images were taken with scanning electron microscopy (SEM, Zeiss Supra 50 VP) at the samples's fractured surfaces. A full profile interpretation by Rietvelt refinement was carried out with the GSAS-EXP GUI software package.

**Table 3.** Seger analysis of the glaze recipes

BCG 01	0.17 Na <sub>2</sub> O			
	0.01 K <sub>2</sub> O	0.42 Al <sub>2</sub> O <sub>3</sub>		
	0.75 CaO		3.62 SiO <sub>2</sub>	8.58 SiO <sub>2</sub> /Al <sub>2</sub> O <sub>3</sub>
	0.07 MgO			
BCG 02	0.17 Na <sub>2</sub> O			
	0.01 K <sub>2</sub> O	0.40 Al <sub>2</sub> O <sub>3</sub>		
	0.75 CaO		3.65 SiO <sub>2</sub>	9.02 SiO <sub>2</sub> /Al <sub>2</sub> O <sub>3</sub>
	0.07 MgO			
BCG 03	0.17 Na <sub>2</sub> O			
	0.01 K <sub>2</sub> O	0.39 Al <sub>2</sub> O <sub>3</sub>		
	0.75 CaO		3.68 SiO <sub>2</sub>	9.49 SiO <sub>2</sub> /Al <sub>2</sub> O <sub>3</sub>
	0.07 MgO			
BCG 04	0.17 Na <sub>2</sub> O			
	0.01 K <sub>2</sub> O	0.37 Al <sub>2</sub> O <sub>3</sub>		
	0.75 CaO		3.71 SiO <sub>2</sub>	10.01 SiO <sub>2</sub> /Al <sub>2</sub> O <sub>3</sub>
	0.07 MgO			
BCG 05	0.17 Na <sub>2</sub> O			
	0.01 K <sub>2</sub> O	0.35 Al <sub>2</sub> O <sub>3</sub>		
	0.75 CaO		3.74 SiO <sub>2</sub>	10.58 SiO <sub>2</sub> /Al <sub>2</sub> O <sub>3</sub>
	0.07 MgO			
BCG 06	0.17 Na <sub>2</sub> O			
	0.01 K <sub>2</sub> O	0.34 Al <sub>2</sub> O <sub>3</sub>		
	0.75 CaO		3.76 SiO <sub>2</sub>	11.20 SiO <sub>2</sub> /Al <sub>2</sub> O <sub>3</sub>
	0.07 MgO			

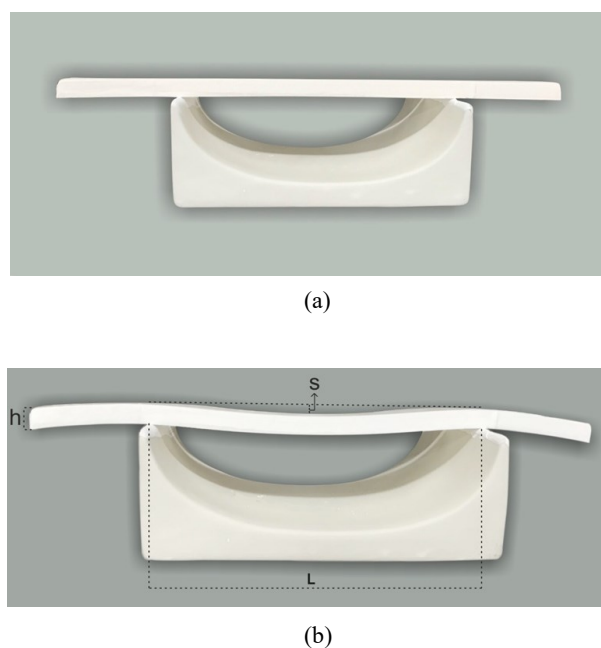


**Fig.1.** Positioning of the sample before (a) and after (b) firing for pyroplastic index assay

### 3. RESULTS AND DISCUSSION

XRD analysis results of the bone china body without glaze after fired at HT1 and HT2 were given in Fig 2. Anorthite ( $\text{CaO} \cdot \text{Al}_2\text{O}_3 \cdot 2\text{SiO}_2$ ) was the primary crystalline phase and the other crystalline phase was whitlockite ( $\text{Ca}_9\text{Mg}(\text{PO}_4)_6(\text{HPO}_4)$ ). The formation of anorthite in the whiteware compositions depends on the composition and also the amount of the source of CaO in the composition. Another important parameter is the firing conditions. [10]. Whitlockite occurs in dental calculi and other abnormal calcifications in the human body, and also has been found in terrestrial rocks and ostensibly in meteorites [11]. It is thought that the existence of whitlockite in the microstructure was related to the existence of bone ash as the source of CaO, MgO and  $\text{P}_2\text{O}_5$  and also the water that used for preparing the body slurry. According to Bronsted-Lowry theory, an acid is a proton donor and a base is a proton acceptor. So the base takes up proton while the acid gives up the proton. Due to the amphoteric properties of water, it acts as a proton donor and a proton acceptor and, the hydrogen ion is simply a proton.

Nonmetal oxide react with water to produce an acidic solution [12].  $\text{P}_2\text{O}_5$  is a nonmetal oxide and it produces an acidic solution with water and hydrogen ion is released from this reaction. During firing, whitlockite ( $(\text{PO}_4)_6\text{PO}_3\text{OH}$ ) formed due to the reactions between CaO, MgO,  $\text{P}_2\text{O}_5$  and  $\text{H}^+$ .

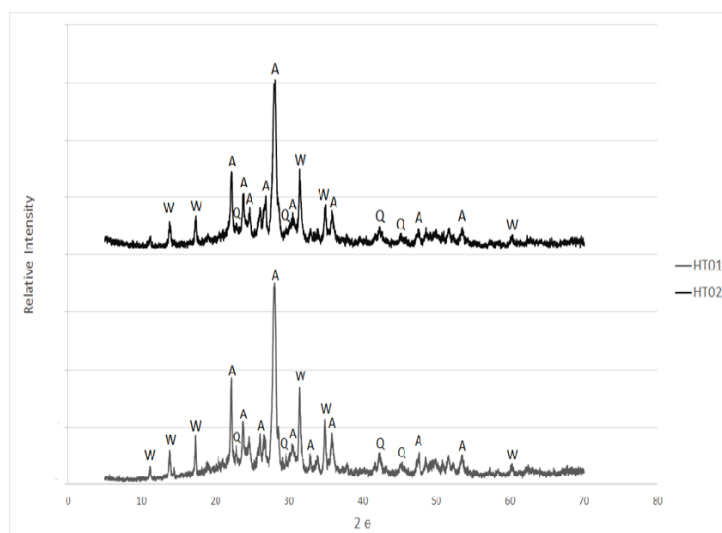


**Fig. 2.** XRD patterns (A: anorthite, W: wicklockite, Q: quartz)

The Reitveld analysis results of the fired bodies were given in Table 4. As the dwelling time increased from 40 minutes to 80 minutes, amount of anorthite and whitlockite decreased because of the crystal's dissolution. Gungor [10] also indicated that formed anorthite was dissolved in the glassy phase when the dwelling time was prolonged. Though the maximum temperature that the samples fired at HT01 and HT02 was the same, holding time at the maximum temperature were different. According to Seger rings, the temperature that the body exposed at the maximum temperature was 1258 °C for HT01 and 1264 °C for HT02. The calculation for determining the viscosity was done by this temperature values. Viscosities of the glassy phases were also given in Table 5. The viscosity of the glassy phase in the sample that fired at HT02 lower than the sample fired at HT01. Although the amount of  $\text{SiO}_2$  and  $\text{Al}_2\text{O}_3$  in the glassy phase increased while anorthite dissolves, in the meantime amount of CaO and MgO also increased.

**Table 4.** Rietveld analysis results of the samples,

	Rietveld analysis				Glassy phase viscosity (logPa*s)
	Quartz	Anorthite	Whitlockite	Amorphous (Glassy)	
*BC/HT01	12.27	34.17	16.21	37.35	4.284
*BC/HT02	11.39	32.11	14.32	42.18	3.937

\* BC/HT01\* Bone China body fired at HT01, \* BC/HT02\* Bone China body fired at HT02.

The thermal expansion coefficient (CTE) results of the glazes fired at HT01 was given in Table 5. CTE of the glazes were increased as the content of  $Al_2O_3$  increased and  $SiO_2$  decreased in the glaze composition. CTE of the body was  $53.2 \times 10^{-6}/^{\circ}C$ . CTE difference between the glaze and body decreases as the content of  $Al_2O_3$  increased in the glaze composition. A glaze will be in a state of compression if it has a lower coefficient of thermal expansion than the body. As a glazed white ware piece is cooling after it has been fired, stresses build up in the glaze and body due to the thermal expansion mismatch between the two. The body wants to contract more than the glaze, which causes the glaze to be placed in compression and the body in tension. This should cause an increase in strength because ceramics break when placed in tension. If the glaze is placed in too much compression, however, shivering can occur. When the glaze has a higher coefficient of thermal expansion than the body, the glaze is placed in a state of tension and a result called crazing can occur. [13, 14]. In this study, there was no crazing problem after firing. CTE difference between bone china glaze and body could be until 10,1% (the difference between the body and the glaze with the lowest CTE, BCG06) and in the further studies, an optimum difference of CTE between bone china glaze and body should be studied. The pyroplastic deformation results of the samples were given in Table 6. As the difference in thermal expansion between the glaze and the body increased, the samples's pyroplastic index increased. However when the CTE of glaze decreases, it is in compression. From this point, it could be specified that the thermal expansion of the glaze did not affect the increasing pyroplastic deformation. SEM images of the samples were given in Fig. 2. Bubble intensities of the glazes increased as the rate of  $SiO_2/Al_2O_3$  in the glaze increased. A lower surface tension favors the release and removal of gas bubbles during the heat treatment of glaze, a higher surface tension will favour the increase of the bubbles during the cooling of glaze [15].

Small increments of alumina have marked effects upon the maturity temperature, the viscosity and surface tension of the glaze, increasing all [16].

**Table 5.** Thermal expansion coefficient (CTE) results of the glazes and standard deviation values

Sample	$\alpha_{500 \times 10^{-7}} (K^{-1})$	$\sigma$
BCG 01	50.7	0.1
BCG 02	50.3	0.0
BCG 03	49.8	0.1
BCG 04	49.1	0.1
BCG 05	48.5	0.0
BCG 06	47.6	0.1

However in this study, in contrast to this information, bubble concentration increased as the amount of  $Al_2O_3$  decreased. Heat microscopy analysis was performed to investigate the cause of this contrast. Heat microscopy analysis results of the samples were given in Fig 3. The start of melting temperatures of the samples of BCG01 and BCG06 were 1194 and 1228  $^{\circ}C$  respectively. The end of melting temperatures of the samples of BCG01 and BCG06 were 1257 and 1273  $^{\circ}C$  respectively. As obtained by seger rings, glazes were exposed to 1258  $^{\circ}C$  for HT01 and 1264  $^{\circ}C$  for HT02. The higher temperature significantly decreases the glaze's viscosity and thereby increase the buoyancy of the gas bubbles, which rise more rapidly and sweep many of the smaller bubbles along [16].

The viscosities of the glazes fired at HT01 and HT02 were given in Fig 4. Viscosities of the glazes increased for both the samples that fired at HT01 and HT02 as the amount of  $Al_2O_3$  increased. Therefore, the increase in the amount of  $Al_2O_3$  has made the zone more refractory and reduced the amount of the bubbles. Bubble population is influenced by the glaze and body composition and by choice of batch materials. Interaction layers, when in the glassy liquid state can also be expected to have different viscosities and surface tensions and consequently to release bubbles in the system at very different rates [17]. Flux migration from the glaze into the body would tend to retard the fusion of the interfacial zone behind the surface [16]. Therefore the same glaze fired on different bodies can give quite different surface qualities [17]. For a better understanding of the effect of body and glaze interaction on the bubble population of the glaze, it is useful to make a systematic study by changing the glaze and body compositions together. The pyroplastic index results of the samples that fired at HT01 and HT02 were given in Table 6. Pyroplastic deformation of the samples fired at HT02 were higher than the samples fired at HT01. As indicated in XRD and Rietveld analysis results, relative intensities of the crystalline phases fired at HT01 were higher than the sample fired at HT02. It indicated that the amount of glassy phase of the sample fired at HT02 was higher than the sample fired at HT01. Glassy phase in the whiteware body, which is a viscous liquid at high temperatures, responsible for undesired shape distortion at high temperature [18]. The pyroplastic deformation increased as the dwelling time increase due to the increased glassy phase and decreased amount of anorthite and whitlockite.

The thickness of the interlayers was measured using SEM and the results revealed that as the rate of  $SiO_2/Al_2O_3$  decreased, the thickness of the interlayer also decreased. Increased interlayer thickness caused an increase in pyroplastic deformation. As the amount of glaze penetrated into the body increased, amount of the glassy phase increased in the body and consequently the tendency of pyroplastic deformation increased. Kara et al [17] indicated that interlayer composition changes as a result of subsequent diffusion of chemical species from glaze into the body and vice versa.

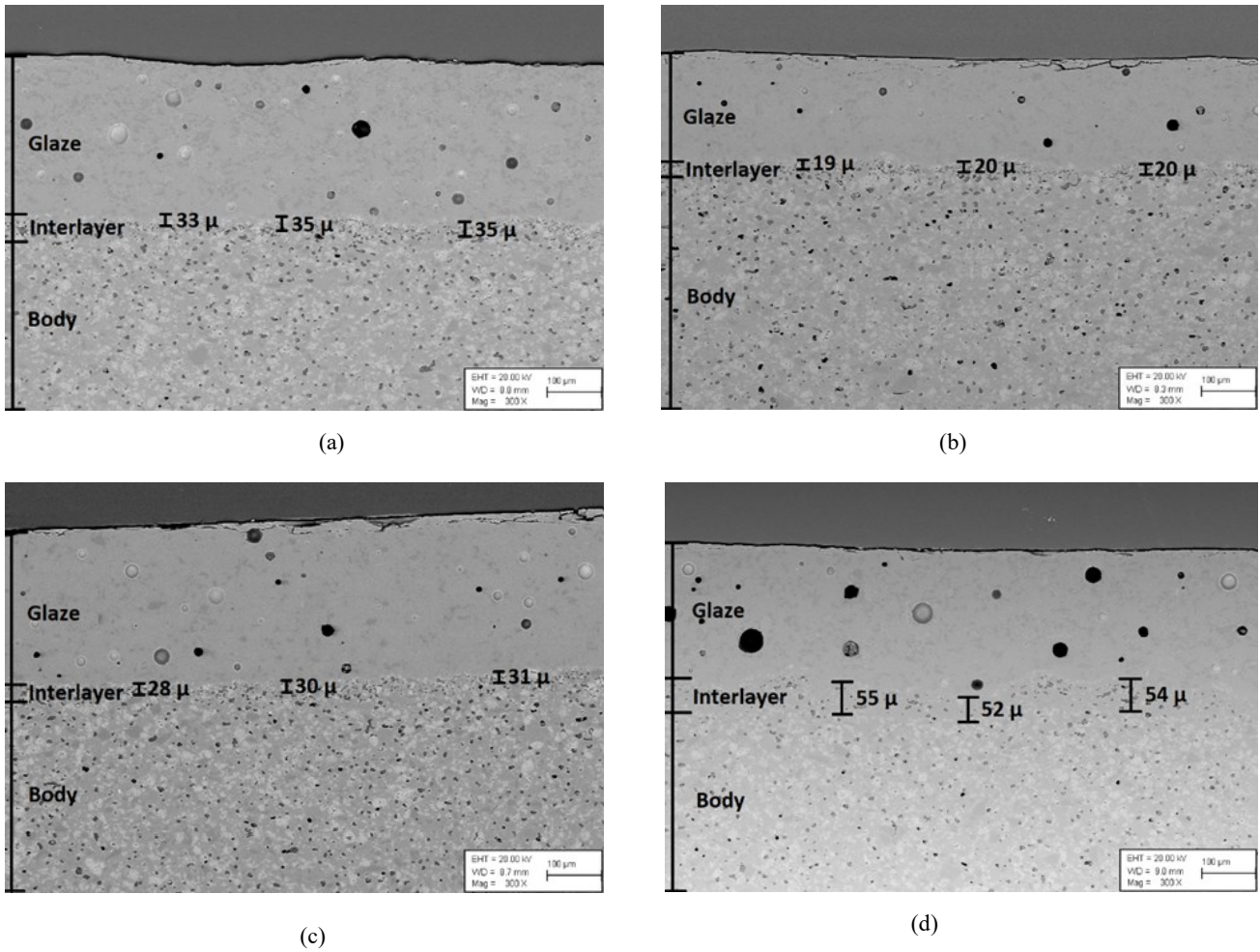


Fig. 3. SEM images of the samples (a) BCG 06 fired at HT01, (b) BCG 01 fired at HT02, (c) BCG 04 fired at HT02, (d) BCG 06 fired at HT02

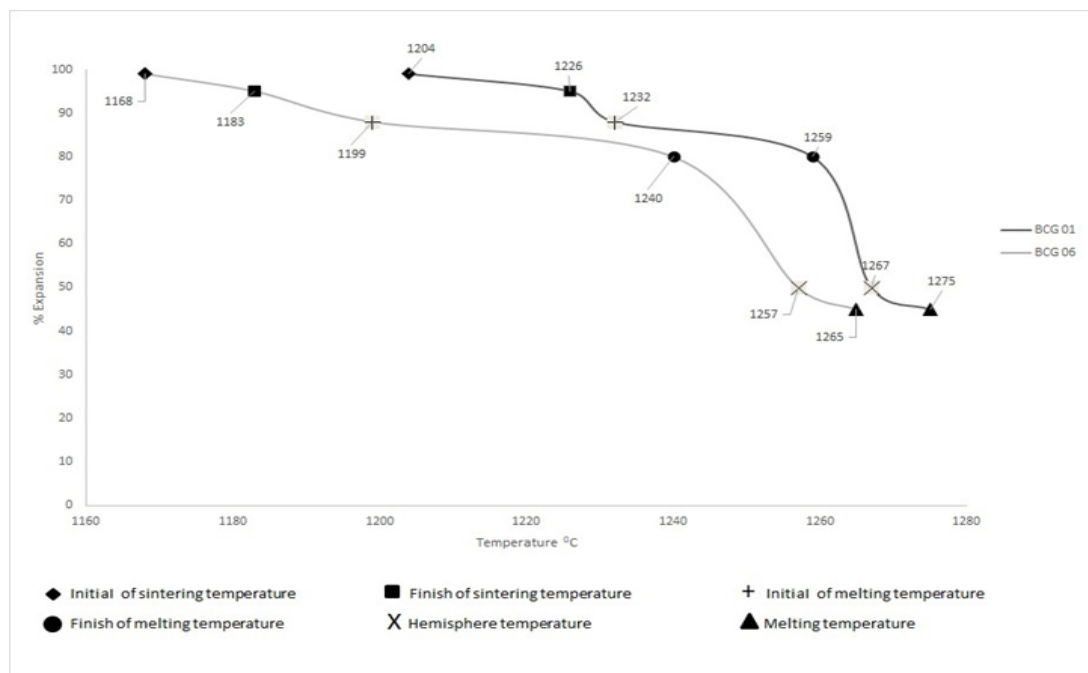


Fig. 4. Heat microscopy analysis of the glazes of BCG01 and BCG06.

**Table 6.** The pyroplastic index results of the unglazed and glazed samples and standard deviation values

Body/Glaze	Heat Treatment	PI ( $\text{cm}^{-1}(10^{-5})$ )	$\sigma$
BC/BCG 01	HT01	4.75	0,117
	HT02	5.42	0,105
BC/BCG 02	HT01	4.91	0,109
	HT02	5.49	0.166
BC/BCG 03	HT01	4.98	0.104
	HT02	5.57	0.146
BC/BCG 04	HT01	5.11	0.115
	HT02	5.71	0.095
BC/BCG 05	HT01	5.39	0.119
	HT02	5.92	0.124
BC/BCG 06	HT01	5.37	0.131
	HT02	6.21	0.069

Glaze viscosity during the firing process was the parameter that determines the rate of penetration of the glaze to the substrate. The results of the calculated viscosities of the glazes were given in Fig 5. The viscosities of the glazes increased as the rate of  $\text{SiO}_2/\text{Al}_2\text{O}_3$  decreased. In the contact zone between the body and the glaze, the original raw products are no longer stable; a reaction occurs which favors the incorporation of atoms from the glaze into the body and from the body to glaze, diffusion being the mechanism responsible

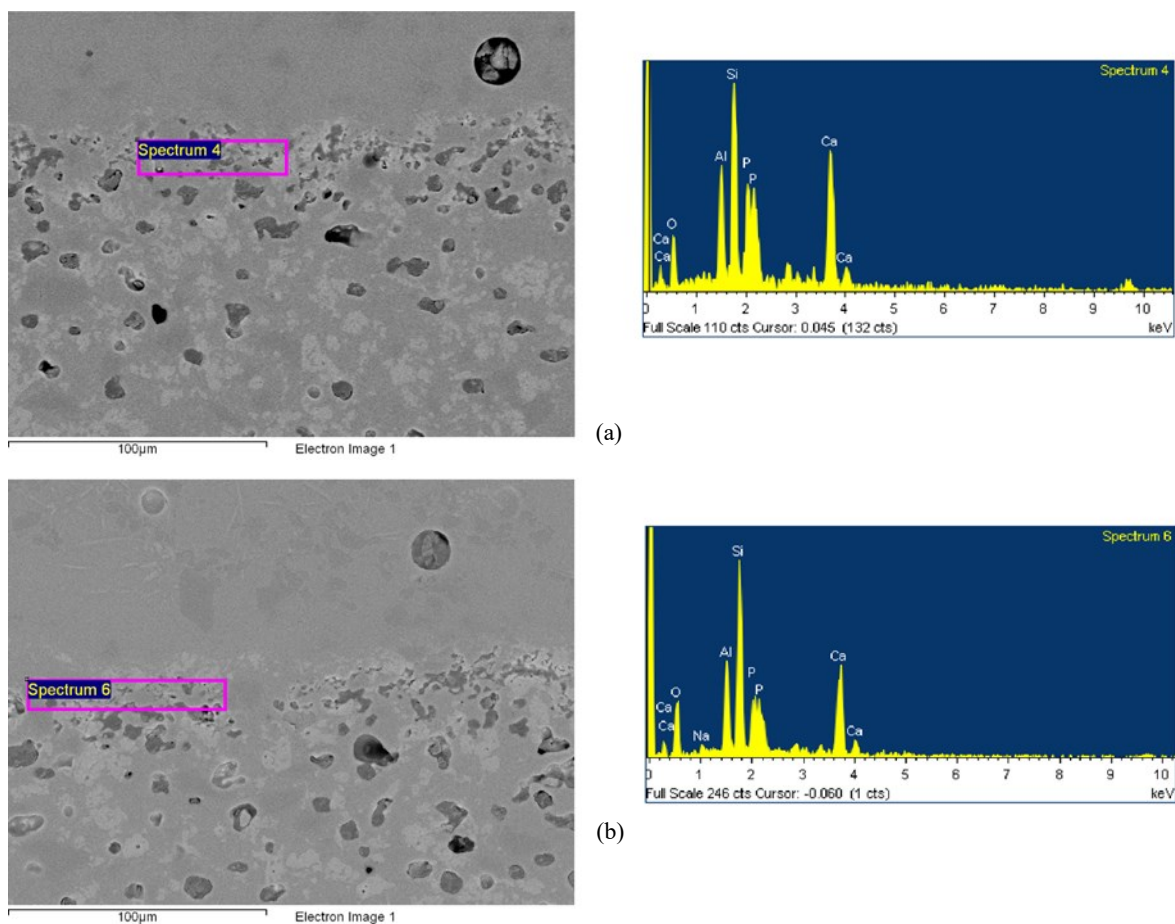
for such migration elements [2, 3]. During firing, as the glaze's viscosity decreased, the glassy phase's viscosity in the interlayer decreased and the crystalline phases in the microstructure of the body dissolved and the amount of the glassy phase and also the thickness of the interlayer increased and pyroplastic deformation increased.

#### 4. Conclusion

The anorthite and whitlockite crystals in the composition of the body dissolved in the glassy phase due to the elongation of the dwelling time at 1250 °C. With the dissolution of the crystals, amount of the glassy phase increased and the deformation tendency of the body increased.

The tension that the body was exposed change as the result of the changed in the thermal expansion coefficient difference between the glaze and the body. The thermal expansion coefficient of the glazes increased as the amount of  $\text{Al}_2\text{O}_3$  increased and  $\text{SiO}_2$  decreased in the glaze composition and the difference between the CTE of the glaze and the body decreased.

Despite the constant composition of the body, the samples coated with different glazes exhibited different pyroplastic deformation behavior at the same firing cycle. At this point, the determining factor is the "interlayer". Interlayer composition and also thickness changed according to the composition of the glaze and the body. The interlayer composition was also a determinant for creep behavior by affecting the viscosity of the glassy phase and as much as the amount of liquid phase formed in the microstructure of the bone china body during firing.


**Fig. 5.** EDX result of the samples of (a) BCG01 and (b) BCG06

In this study, due to the changed glaze composition and heating cycle, the composition of the interlayer between the glaze and the body changed. As a result of changed interlayer composition, the thickness of the interlayer changed because the penetration capacity of interlayer throughout to the body increased as the rate of SiO<sub>2</sub>/Al<sub>2</sub>O<sub>3</sub> increased in the glaze composition. As the thickness of interlayer increased, the pyroplastic deformation of bone china also increased.

## References

1. S. Ke, Cheng X., Wang Y., Wang Q., Wang H., "Dolomite, wollastonite and calcite as different CaO sources in anorthite based porcelain", *Ceramics International*, **39** (5) 4953-4960 (2013).
2. E. Thomas, Tuttle M.A., Miller E., "Study of Glaze penetration and its effect on glaze fit: I-III", *Journal of the American Ceramic Society*, **28** (2) 52 - 62 (2006).
3. D. Sighinolfi, "Experimental study of deformations and state of tension in traditional ceramic materials", *Ceramic Materials*, **63** (2) 226-232 (2011).
4. J. Benson, "Effect of glaze variables on the mechanical strength of whitewares", *B.S. Thesis*, Alfred University, (2003).
5. W.D. Kingery, Bowen H.K., Uhlmann D.R., *Introduction to Ceramics*, John Wiley & Sons Inc., New York, (1976).
6. A. Salem, Jazayeri S.H., Rastelli E., Timellini G, "Dilatometric study of shrinkage during sintering process for porcelain stoneware body in presence of nepheline syenite", *Journal of Materials Processing Technology*, **209** (3) 1240-1246 (2009).
7. P. Rado, "Bone china", *Ceramics Monographs – A Handbook of Ceramics*, Verlag Schmidt GmbH, Freiburg i. Brg., (1982).
8. T. Lakatos, Johansson L.G., Simmingsköld B., "Viscosity temperature relations in the glass system SiO<sub>2</sub>-Al<sub>2</sub>O<sub>3</sub>-Na<sub>2</sub>O-K<sub>2</sub>O-CaO-MgO in the composition range of technical glasses", *Glass Technology*, **13** (3) 88–95 (1972).
9. L. Conserva, Melchiades F., Nastri S., Boschi A., Dondi M., Guaribi G., Raimondo M., Zanelli C., "Pyroplastic deformation of porcelain stoneware tiles: Wet vs., dry processing", *Journal of the European Ceramic Society*, **37** (1) 333-342 (2017).
10. F. Gungor, "Investigation of pyroplastic deformation of white-ware: Effect of crystal phases in the "CaO" based glassy matrix", *Ceramics International*, **44** (11) 13360–13366 (2018).
11. J.M. Hughes, Jolliff B., Rakovan J., "The crystal chemistry of whitlockite and merrillite and the dehydrogenation of whitlockite to merrillite", *American Mineralogist*, **93** (8-9) 1300-1305 (2008).
12. R.H. Petrucci, Herring F. G., Madura J. D., Bissonnette C., *General Chemistry Principle and Modern Applications*, 10<sup>th</sup> Edition, Pearson Canada Inc., Toronto, (2011).
13. C. Radford, "A New Instrument for Assessing Body/Glaze Fit", *British Ceramic Transactions*, **76** (3) 20-25 (1977).
14. B. Plesingerova, Kovalcikova M., "Influence of the thermal expansion mismatch between body and glaze on the crack density of glazed ceramics", *Ceramics-Silikaty*, **47** (3) 100-107 (2003).
15. R.L. Dumitrache, Teoreanu I., "Melting Behaviour of Feldspar Porcelain Glazes" *U.P.B. Sci. Bull., Series B*, **68** (1) 3-16 (2006).
16. C.W. Parmelee, *Ceramic Glazes*, Ind. Pub., Chicago, USA, (1948).
17. A. Kara, Stevens R., "Interaction between an ABS type leadless glaze and a biscuit fired bone body during glost firing", *Journal of the European Ceramic Society*, **22** (7) 1095-1102 (2002).
18. L.R.S. Conserva, Melchiades F.G, Nastri S., Boschi A.O., Dondi M., Guarini G., Raimondo M., "Pyroplastic deformation of porcelain stoneware tiles: wet vs. dry processing", *Journal of the European Ceramic Society*, **37** (1) 333–342 (2017).